5286 J. Agric. Food Chem. 2010, 58, 5286–5291
DOI:10.1021/jf100436c

JOURNAL OF AGRICULTURAL AND FOOD CHEMISTRY
ARTICLE

Leather Structure Determination by Small-Angle X-ray Scattering (SAXS): Cross Sections of Ovine and Bovine Leather

Melissa M. Basil-Jones,[†] Richard L. Edmonds,[§] Timothy F. Allsop,[§] Sue M. Cooper,[§] Geoff Holmes,[§] Gillian E. Norris,[‡] David J. Cookson,[⊥] Nigel Kirby,[⊥] and Richard G. Haverkamp*,[†]

[†]School of Engineering and Advanced Technology, and [‡]Institute of Molecular Biosciences, Massey University, Palmerston North, New Zealand 4442, [§]Leather and Shoe Research Association, Palmerston North, New Zealand 4442, and [⊥]Australian Synchrotron, Melbourne, Australia

SAXS has been applied to structural determination in leather. The SAXS beamline at the Australian Synchrotron provides 6 orders of magnitude dynamic range, enabling a rich source of structural information from scattering patterns of leather sections. SAXS patterns were recorded for q from 0.004 to 0.223 Å^{-1}. Collagen d spacing varied across ovine leather sections from 63.8 nm in parts of the corium up to 64.6 nm in parts of the grain. The intensity of the collagen peak at q = 0.06 Å^{-1} varied by 1 order of magnitude across ovine leather sections with the high-intensity region in the corium and the low intensity in the grain. The degree of fiber orientation and the dispersion of the orientation has been quantified in leather. It is shown how the technique provides a wealth of useful information that may be used to characterize and compare leathers, skin, and connective tissue.

KEYWORDS: Leather; small-angle X-ray scattering; SAXS; synchrotron; ovine; bovine; fiber structure; collagen

INTRODUCTION

The value of leather depends on the physical and aesthetic properties of the material. The leather industry is large, with global production of about 1.7 billion square meters of leather per year with a value of around $40 billion. About 65% of the world production of leather goes into footwear, worth an estimated $150 billion at wholesale prices. Other major uses include upholstery (including automotive) and clothing.

The properties of leather ultimately depend on the properties of the component fibers and their structure. Leather consists of a network of collagen fibrils interlinked with natural and synthetic chemical bonds. The collagens are a group of proteins that are responsible for providing structure and desirable physical properties to a number of tissues in the body (*1*).

Collagen is almost always present in its characteristic hierarchical structure (*2*). At its primary level, pro-collagen molecules are characterized by the repetitive chain sequence of $(Gly\text{-}X\text{-}Y)_n$, where Gly is glycine, X and Y can be any amino acid, and n is the number of repeats, usually 100−400 (*3*). A collagen molecule is composed of three of these chains, which combine in a coiled-coil structure, due to the chain's repetitive sequence. These molecules align to form microfibrils, in a quarter-staggered array which results in the formation of overlap and gap regions. These regions are responsible for the characteristic banding pattern observed in collagen fibrils with atomic force or scanning electron microscopy. The period of this repeating sequence is known as the d period. The microfibrils arrange in a parallel fashion and through cross-links form collagen fibrils.

Collagen fibril arrangement can vary significantly between different tissues. In skin, collagen fibrils tend to have a low variation in diameter (*4*) and form a random web-like structure (*5*). It has been found that many collagens, in particular type I, III, and VI collagens, are resistant to liming, bating, and pickling (*6*). Collagen fibrils have a large inherent strength, and the arrangements of collagen fibrils are crucial to the final physical properties of the leather. The strength and softness of leather are believed to be related to the internal structure of the leather (*7*, *8*) and aesthetic properties to the internal fiber looseness (*9*).

Leather has a complex hierarchical structure with a number of distinct layers. The grain layer found at the leather outer surface and the corium layer found beneath have visually different structures and impart different properties to the final leather (*10*). The physical properties of those layers are strongly related to the fiber structure of which they are made up. The organization of these layers and the resulting physical properties are also influenced by cross-linking, either natural or modified (*11*−*14*).

Differences between fiber structures have been determined through the use of optical microscopy, scanning electron microscopy (SEM) (*15*−*19*), and atomic force microscopy (AFM) (*18*, *20*, *21*). The microscopic techniques generally give qualitative measurement of fiber organization but may also give quantitative measurement of fiber dimensions and d period.

*To whom correspondence should be addressed. E-mail: r.haverkamp@massey.ac.nz.

 Published on Web 03/25/2010

X-ray diffraction is a powerful technique for investigating material structures. The study by X-ray diffraction techniques of long-range structural order, with repeat distances on the order of 0.1−10 nm, is particularly useful for protein assemblages, such as collagen. Such measurements require small diffraction angles, θ, typically less than 10 degrees and are often referred to as small angle X-ray scattering (SAXS). The scattering momentum q ($q = 4\pi(\sin\theta)/\lambda$, where λ is the X-ray wavelength used) is generally used rather than θ in SAXS plots, as it allows direct comparison of SAXS measured at different incident X-ray wavelengths. SAXS can provide information on macromolecules either in solution or in solid materials (*22*, *23*) and has been used to investigate the structure of collagen (*24*) and collagenous materials such as tendon (*2*, *25*), bone (*26*, *27*), and human articular cartilage (*28*). SAXS provides a quantitative measurement of both fibril orientation and the average d spacing of collagen within the irradiated volume of sample.

Leather has previously been investigated using SAXS. Fiber orientation was identified in leather samples under strain (*29*, *30*), although in these studies the resolution appears to be rather limited with collagen d period not easily observed in the diffraction patterns.

In this work, we describe how modern high-sensitivity SAXS may be applied to the study of leather using the wealth of information available in a two-dimensional SAXS pattern. We describe the use of some of this information and show, using examples, how it may be applied to characterize leather. Some of this information can be directly related to existing industry tests, while other information is new to the field. The use of these techniques to infer important structural differences in different leathers will be the subject of subsequent publications.

EXPERIMENTAL SECTION

SAXS diffraction patterns were recorded on the Australian Synchrotron SAXS/WAXS beamline, utilizing a high-intensity undulator source. An energy resolution of 10^{-4} is obtained from a cryo-cooled Si(111) double-crystal monochromator, and the beam size (fwhm focused at the sample) was $250 \times 80\ \mu$m with a total photon flux of about 2×10^{12} photons s^{-1}. All diffraction patterns were recorded with an X-ray energy of either 8 or 11 keV using a Pilatus 1 M detector with an active area of 170×170 mm and a sample to detector distance of 3371 mm. The exposure time for diffraction patterns was in the range of 1−5 s, and data processing was carried out using the SAXS15ID software (*31*). Intensities displayed are all absolute detector counts (one X-ray detected one detector count), except where stated otherwise.

Leather was prepared from pelt leather using conventional beamhouse and tanning processes. Briefly, the pelts were depilated using a caustic treatment comprising sodium sulfide and a saturated solution of calcium hydroxide followed, after washing, by pickling in sulfuric acid and sodium chloride to a pH of less than 2. The pickled pelts were then pretanned using oxazolidine, degreased with an aqueous surfactant, and then tanned using chromium sulfate. The resulting "wet blue" was then retanned using a mimosa vegetable extract and impregnated with lubricating oil prior to drying and mechanical softening.

Strips of leather about 1 mm thick and 30 mm long were cut at selected positions from samples of tanned ovine and bovine leather. The leather was mounted in the beam horizontally without tension. Samples were mounted on a support which held up to 36 samples and which could be manipulated remotely, which enabled rapid profiling across a sample of leather and quick sample changing (**Figure 1**).

Analyses were performed across the section of each strip of leather starting at the region of the grain and progressing through to the corium (**Figure 2**). Steps of either 0.25 or 0.05 mm were made between analysis points. The rectangles shown on **Figure 2** show the beam probe size and scan spacing, demonstrating that the smaller step size was comparable with the fwhm of the beam at the sample. Analyses were also performed normal to the surface of the leather.

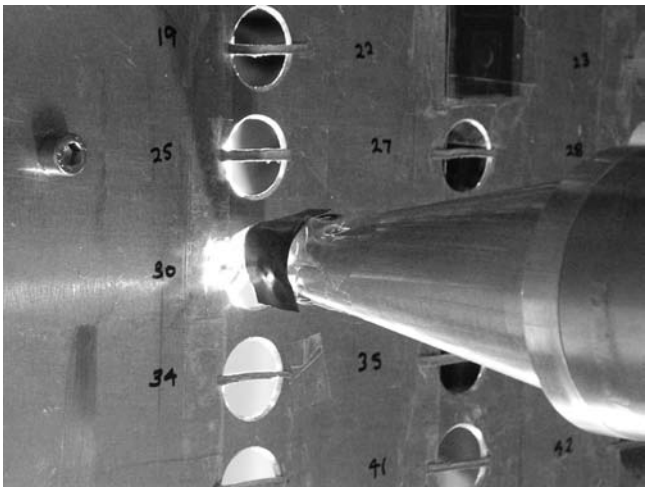

Figure 1. Image of leather samples mounted on sample holder with camera entrance cone in position. Holes are 25 mm diameter.

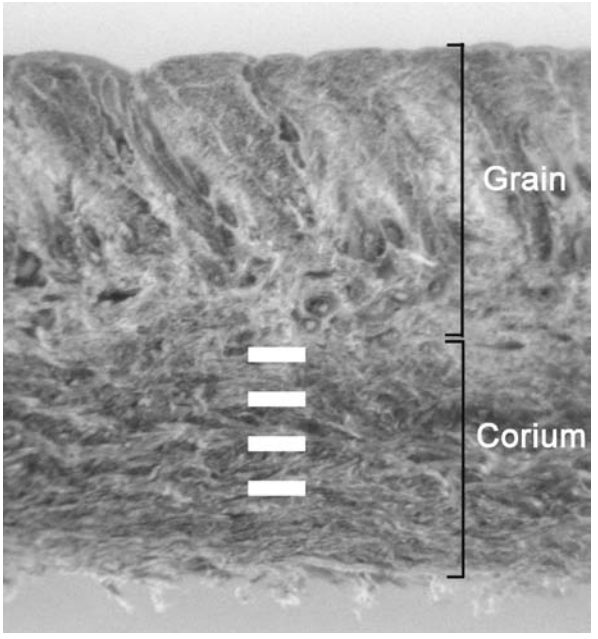

Figure 2. Optical image of a cross section of ovine leather as seen by the SAXS X-ray beam. The height (leather thickness) of the section shown is 2.2 mm but varies between samples. The rectangles indicate the size of the beam used to probe the sample (shown at 0.25 mm spacing, for 0.05 mm spacing the analysis area overlaps by 30%).

Thin sections parallel to the surface of the leather were also made by sectioning the leather strips into three layers, one containing just grain, one with the middle part, and one with just corium. These were mounted with the face of the leather toward the X-ray beam.

RESULTS AND DISCUSSION

Diffraction Pattern. Diffraction images of leather recorded on Pilatus detector with the Australian Synchrotron provide remarkable resolution (**Figure 3**). Previous synchrotron SAXS studies failed to show the same level of detail (*29*, *30*). However, on the data recorded on the Pilatus detector it is possible to record across

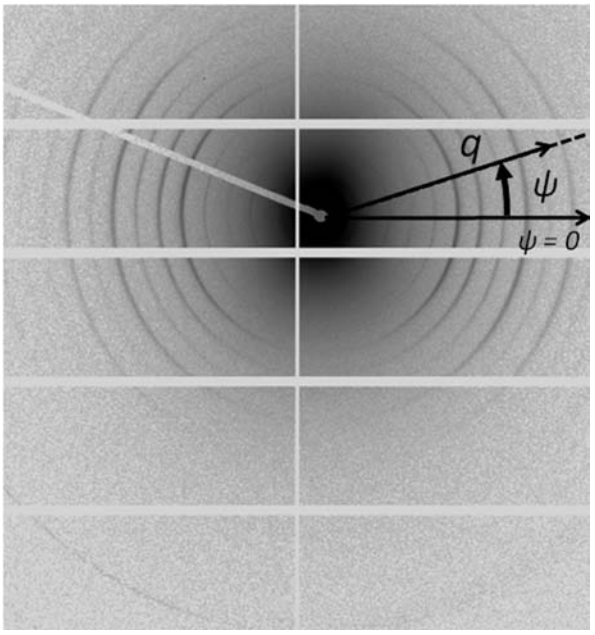

Figure 3. SAXS image of ovine leather. The image extends to q = 0.223 A^{-1} at the bottom left-hand corner. Note that q is calculated from the scattering angle and that the azimuthal angle ψ is measured anticlockwise from the horizontal.

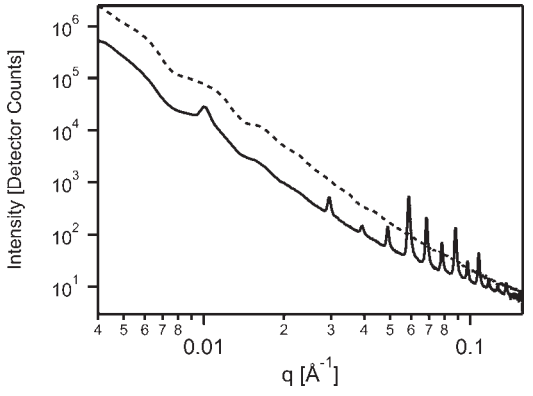

Figure 4. SAXS profiles of an example of ovine leather using two azimuthal angle ranges. The dashed line shows profiles integrated from ψ = 60 to 120°, while the solid line shows ψ = −30 to 30°.

6 orders of magnitude of intensity enabling the Bragg peaks from the collagen d period to be easily observed (at q = 0.04−0.1 $Å^{-1}$) while simultaneously measuring to low q (0.004 $Å^{-1}$), where the signal intensity is much greater (**Figure 4**).

From a single SAXS image taken of a leather sample, information relating to fiber and fibril structure, collagen concentration, and orientation can be readily obtained. The positions of the series of prominent rings correspond to the Bragg peaks from the collagen d period, the region at low q yields information on fiber morphology, the intensity of the collagen rings relates to the collagen concentration, the broadness of these rings relates to crystallinity, and the angular distribution of the rings provides information on fibril orientation. We will discuss some of these parameters in turn below. All the figures shown, with the exception of **Figure 10**, are for spectra recorded with the X-ray beam parallel to the original leather surface.

Radial Integration of Scattering Pattern. Most SAXS scattering patterns from leather samples are highly nonisotropic, meaning that a plot of intensity (I) versus q will give significantly different

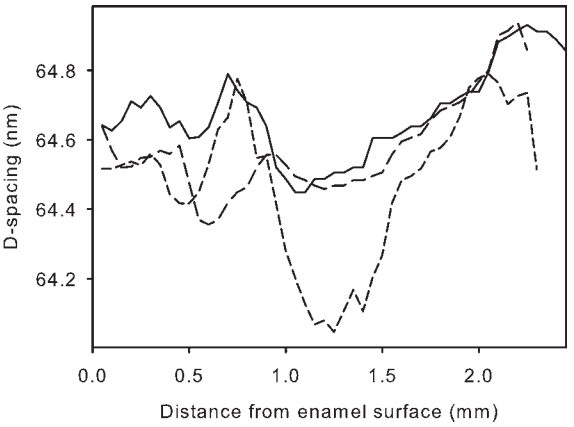

Figure 5. Variation of collagen d period through ovine leather (for three samples).

profiles depending on the azimuthal range of integration. The I versus q profile changes when integrating over the meridional arcs (ψ = −30 to 30°) or over the region without the arcs (ψ = 60 to 120°), as illustrated in **Figure 4**. For the former azimuthal region the profile shows a series of peaks at q in the range 0.04−0.1 $Å^{-1}$ corresponding to periodicity of molecular overlap in the collagen fibrils. Around 15 of these arcs can be observed in the raw diffraction pattern. Measuring the q position for the center of any one of these peaks provides a quantitative measure of the collagen molecule overlap or d period. The sixth Bragg peak was generally used, as it was the most intense, although it was found that any of the other intense peaks would provide the same information.

In addition, structural information can be obtained from the region of low q (below 0.03 $Å^{-1}$). This lower angle region provides information on the larger structures, the fibers in the material (*32*). The slope of this line when plotted on a log−log scale indicates the nature of the boundary between the organized fibers and the disorganized medium. In this case there is a clear oscillation in the profile in both azimuthal regions—with an average envelope slope of 4 ± 0.1 on the log−log plot. This means that the general decay of intensity at lower q goes as q^{-4}, which conforms to Porod's law. A Porod law slope indicates that there is a sharp well-defined (smooth) boundary between the fibrils and their nearest neighboring fibrils and/or surrounding air and amorphous material.

Structure of Collagen. Upon analysis of the position of the collagen peaks (**Figure 4**), a large variation in collagen d period can be observed through the thickness of leather samples (**Figure 5**). The d period is seen to decrease in the corium compared with the grain layer (**Figure 5**). Differences in d period between different tissues has previously been observed, using other methods, with skin having a lower d period (65 nm) than tendon (67 nm) (*5*). The shorter d period is closer to that which we observe here in leather. The differences in d period have proposed to not be related to stretch or crimp but rather may be due to the intrafibrillar texture in the tissues (*5*). It has also been suggested that for collagen with a helical inner structure the d spacing only appears to be shorter due to the projection of this structure along the fibril axis (*4*). The d spacing has been correlated with fibril diameter, with small diameter fibrils having a smaller d period (*4*, *5*).

Reproducibility and Variability. Leather is potentially a nonhomogenous material at the scale of the SAXS analysis (80 μm × 250 μm spot). This can be used to advantage by imaging the variation across a cross section. However, for the simple tests we are presenting here, an assurance is needed that this variation is

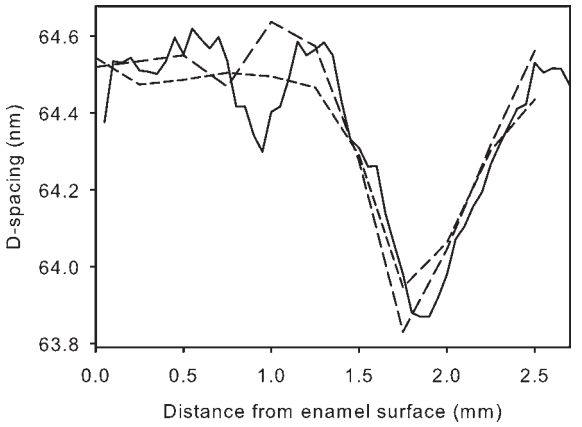

Figure 6. Example of reproducibility of *d* period measurement in adjacent regions on one sample: (solid line) 5 s exposure, 0.05 mm sampling; (dashed lines) 1 s exposure, 0.25 mm sampling.

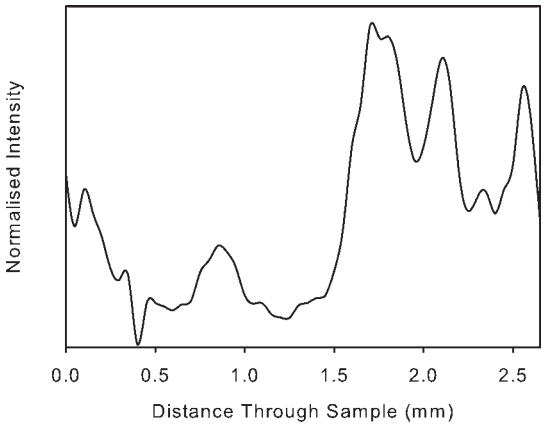

Figure 7. Example of the intensity of the primary collagen *d* spacing peak (at around 0.059−0.06 $Å^{-1}$) through ovine leather, normalized for total scattering at low *q*, taken at 0.05 mm steps. The grain surface is at 0 mm.

not so large as to make a scan of a series of points across the sample nonrepresentative. We have therefore made several point scans across samples and calculated the intensity and *d* period across these scans (**Figure 6**). The variation from one series of points to the next is small compared with the variation across the thickness of the sample or the variation between samples, which gives some confidence that the measurement is useful. Similarly, the orientation parameters are similar from one scan across a section to another on the same sample (not shown).

Concentration of Crystalline Fibrillar Collagen across the Leather. By measuring the intensity (integrated area) of a selected collagen diffraction peak across the profile of the leather sample, it is possible to quantify the concentration of crystalline fibrillar collagen in the sample. First it is necessary to correct for any variation in sample thickness and density across the area of analysis. This can be done by normalizing with respect to the total scattering in the low *q* region. The variation of intensity of the Bragg peaks for collagen observed for a sample of ovine leather (**Figure 7**) is nearly 1 order of magnitude, with the most intense region across the corium, the region known to provide most of the strength to leather (*33*).

It is well recognized that the grain layer of leather is weak compared with the corium, with the grain having perhaps as little as 20% of the tearing strength of corium. It has been suggested that these differences in strength between the two strata of leather are associated with the greater ability of the corium layer's fiber

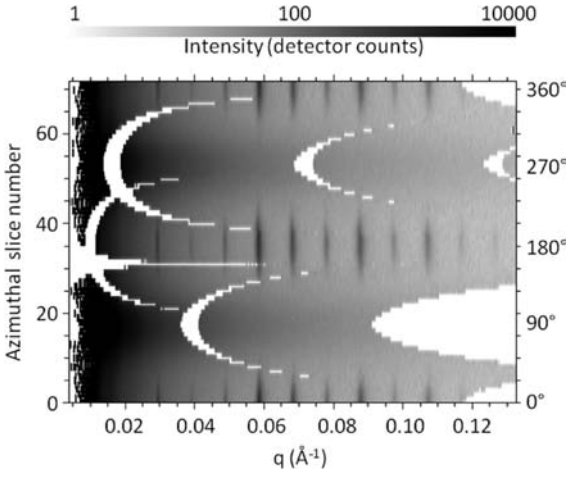

Figure 8. Gray shade plot of *q* versus azimuthal angle for an ovine leather. The white arcs on the left of the image represent the gaps in the detector. The dark vertical bands centered vertically on the azimuth angle of 0 and 180° are the collagen *d* spacing Bragg peaks. SAXS intensity is given by the gray scale.

structure to impede propagating tears by means of tear tip blunting and fiber pull out (*33*). The measure of fibrilar collagen content could therefore be a guide to leather strength, with high concentrations of structured fibrilar collagen corresponding with regions of high strength (**Figure 7**).

It may also be possible to measure the "crystallinity" of the collagen. This can be done by measuring the intensity of the higher order peaks relative to lower order peaks. These higher order peaks would be expected to decay in intensity more quickly when the *d* spacing is poorly conserved. We have not yet investigated this aspect.

Orientation of Collagen. The orientation of collagen fibrils in the plane normal to the irradiating X-ray beam can be obtained from the azimuthal distribution of the diffraction arcs. The samples are taken parallel to the backbone of the animals, and this direction represents 0° on the plots for all samples. For standard samples 90° represents the direction from the grain to the corium. For the thin surface parallel sections 90° is the direction at right angles to the backbone and parallel to the surface.

A series of profiles from azimuthal subregions 5° wide around the entire 360° range of an image can be used to generate a composite image of arcs (vertical dark lines) that can be readily analyzed for intensity, position, and length (**Figure 8**).

By selection of a small enough *q* range a single meridional arc can be selected and analyzed in detail. In **Figure 9** a single meridional arc in the region $q \approx 0.06$ $Å^{-1}$ is compared between example samples of bovine and ovine leather (not the same sample as in **Figure 4**). The arcs from the bovine sample indicate only one preferred direction (a peak at 0 and 180° azimuth), while the arcs in the particular ovine sample shown indicate two preferred directions (peaks at 0, 90, 180, and 270°). Both leather cross-sectional samples were cut parallel to the backbone (0, 180°).

The spread of fibril orientation can be quantified by the width of the peaks in the azimuthal angle plots (**Figure 9**). In the case of the collagen peaks of bovine leather illustrated this was 72° and for ovine illustrated 44° in the primary direction of orientation and 35° for some fibrils at right angles. This particular bovine sample, therefore, could be said to have a greater spread of fibril orientation around the preferred direction than the ovine sample. The ovine sample has a narrower distribution in the preferred direction, but it also has some fibrils running at right angles to the line of the backbone.

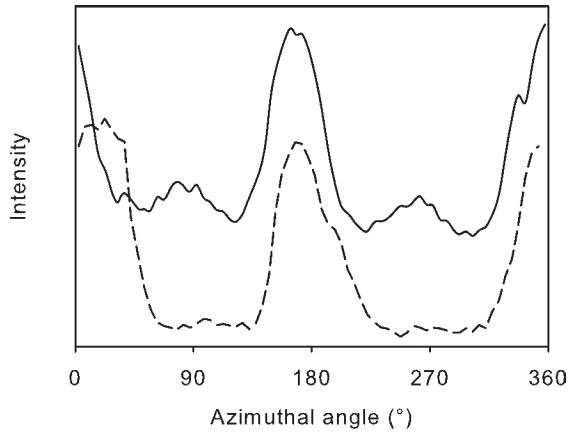

Figure 9. Examples of azimuthal angle plots of bovine leather at ~0.6 $Å^{-1}$ (dashed line) and ovine leather at ~0.6 $Å^{-1}$ (solid line), with arbitrary intensity scale and offset. Note that the narrow dips on the sides of some peaks are artifacts caused by gaps in the detector.

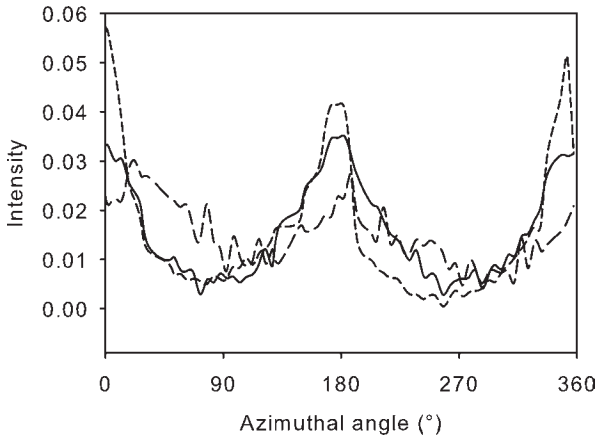

Figure 10. Azimuthal angle plots of ovine leather at the collagen *d* spacing peak around 0.059−0.06 $Å^{-1}$ for SAXS taken of sections parallel to an ovine leather surface: (solid line) grain; (long dash) middle; (short dash) corium. The X-ray beam was normal to the original leather surface.

The sections of leather cut parallel to the leather surface, each about one-third of the thickness of the leather, also show a collagen orientation aligned at 0 and 180° (i.e., parallel to the backbone), as shown in **Figure 10**, but with a greater spread in that plane than in the plane of a cross section (**Figure 9**). The strongest orientation is observed in the corium.

The azimuthal distribution of the collagen diffraction rings can be plotted across the thickness of the leather samples in a three-dimensional representation to visualize the variation of orientation with position in the leather (**Figure 11**). A plot of the absolute magnitude of these diffraction peaks (**Figure 11a**) may be a useful indicator of the possible contribution of the combined effect of the amount of collagen and its orientation on the physical properties of the leather. Or, by normalizing the data at each position to a constant intensity, the effect of varying collagen concentration is removed so that just the orientation data is displayed (**Figure 11b**).

The orientation of the collagen within leather falls into two regions: highly oriented in the corium and poorly oriented in the grain. It is well-known that the corium is stronger than the grain. Therefore, there is a correlation between orientation and strength (as there is between the amount of collagen and strength and between *d* spacing and strength). It may therefore be useful to

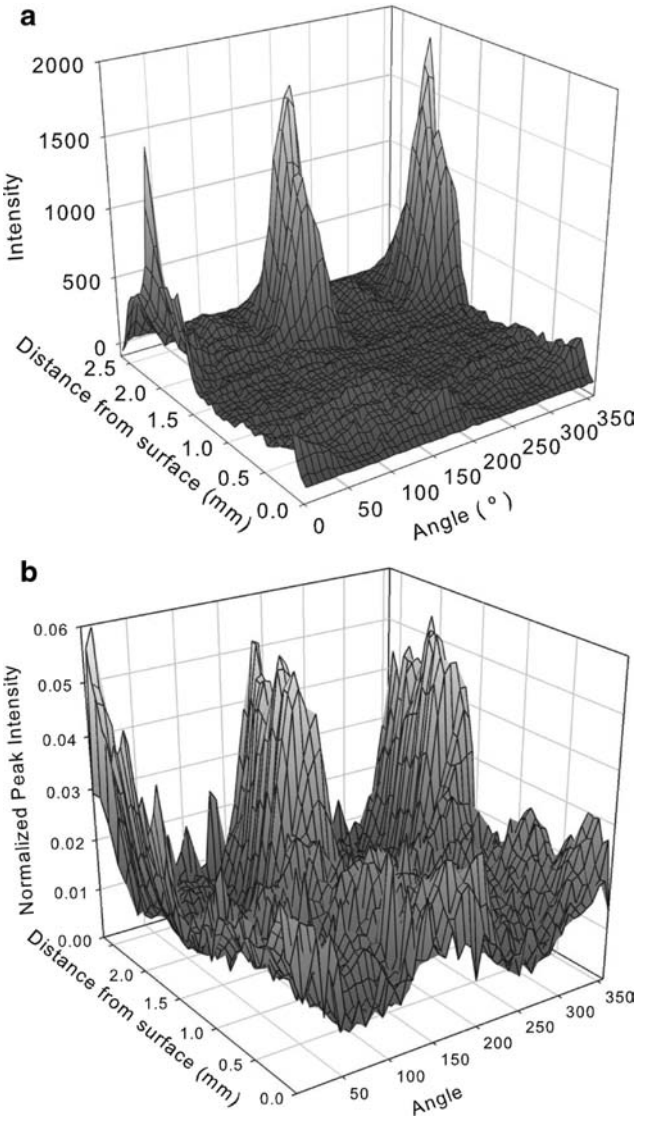

Figure 11. Azimuthal angle through ovine leather at the collagen *d* spacing peak around 0.059−0.06 $Å^{-1}$: (a) absolute intensity; (b) intensity normalized to an equal sum at each sample position, therefore showing only relative orientation.

investigate this correlation to determine if a greater degree of orientation in collagen is a contributing factor for higher strength. This method may provide a more reliable quantitative measure of fiber orientation than the existing industry methods which use optical microscopy to measure individual fiber orientation in samples of leather and therefore have poorer sampling statistics than the SAXS method. These examples given are illustrative only and demonstrate the orientation information that may readily be obtained.

Usefulness of the Technique. Leather is a structured material with clearly measurable differences between the corium and the grain. The corium contains, relative to the grain, a greater concentration of collagen which is more highly oriented and has a shorter *d* spacing. The corium is known to be stronger than the grain (although less elastic), and these measured differences are likely to contribute to the differences in mechanical properties.

We have shown that this technique provides quantitative information on the leather structure. The three parameters we have measured, *d* spacing, collagen orientation, and amount of collagen, all correlate with strength in the samples we have analyzed (*33*). They are therefore confounded and it is not

possible to say with any certainty what each of their individual contributions are to the strength of leather. We are now conducting a detailed SAXS-based comparison of leathers with different physical properties to quantitatively evaluate the relationship between the SAXS-derived parameters and the mechanical properties.

In combination with traditional and emerging testing methods such as light microscopy, scanning electron microscopy, and atomic force microscopy, SAXS provides complementary information that will be increasingly important in the characterization of leather, with the prospect of allowing us insight into how such characteristics could be improved in this complex composite material. Synchrotron SAXS allows these studies to be done quickly, for a wide range of samples and with an unparalleled degree of spatial precision.

ACKNOWLEDGMENT

This research was undertaken on the SAXS/WAXS beamline at the Australian Synchrotron, Victoria, Australia.

LITERATURE CITED

(1) Fratzl, P. *Collagen: Structure and Mechanics*; SpringerScience+ Business Media: New York, 2008.
(2) Sasaki, N.; Odajima, S. Elongation mechanisms of collagen fibils and force-strain relations of tendon at each level of structural hierarchy. *J. Biomech.* **1996**, *29* (9), 1131–1136.
(3) Bailey, A. J.; Paul, R. G. Collagen: a not so simple protein. *J. Soc. Leather Technol. Chem.* **1999**, *82*, 104–110.
(4) Ottani, V.; Raspanti, M.; Ruggeri, A. Collagen structure and functional implications. *Micron* **2001**, *32*, 252–260.
(5) Gathercole, L. J.; Shah, J. S.; Nave, C. Skin-tendon differences in collagen D-period are not geometric or stretch-related artefacts. *Int. J. Biol. Macromol.* **1987**, *9*, 181–183.
(6) Stephens, L. J.; Werkmeister, J. A.; Ramshaw, J. A. M. Changes in bovine hides during leather processing. *J. Soc. Leather Technol. Chem.* **1993**, *77* (3), 71–74.
(7) Russell, A. E. Stress-strain relationships in leather and the role of fibre structure. *J. Soc. Leather Technol. Chem.* **1988**, *72* (4), 121–134.
(8) Michel, A. Tanners' dilemma: Vertical fibre defect. *Leather Int.* **2004**, *206* (4750), 36–37.
(9) Rabinovich, D. Seeking soft leathers with a tight grain. *WORLD Leather* **2001**, *14* (5), 27–32.
(10) Vera, V. D.; Cantera, C. S.; Dominguez, D. O.; Bernardi, C. In *Modern Soft Leather Influence of the Relationship Grain/Corium on the Topography of Some Physical Properties*; 22nd IULTCS Congress Proceedings, Porto Alegra, ABQTIC: Porto Alegre, Brazil, 1993; pp 560−569.
(11) Folkhard, W.; Geercken, W.; Knorzer, E.; Mosler, E.; Nemetschek-Gansler, H.; Nemetschek, T.; Koch, M. H. J. Structural dynamic of native tendon collagen. *J. Mol. Biol.* **1987**, *193*, 405–407.
(12) Folkhard, W.; Geercken, W.; Knorzer, E.; Nemetschek-Gansler, H.; Nemetschek, T.; Koch, M. H. J. Quantitative analysis of the molecular sliding mechanism in native tendon collagen - time-resolved dynamic studies using synchrotron radiation. *Int. J. Biol. Macromol.* **1987**, *9* (3), 169–175.
(13) Chan, Y.; Cox, G. M.; Haverkamp, R. G.; Hill, J. M. Mechanical model for a collagen fibril pair in extracellular matrix. *Eur. Biophys. J. Biophys.* **2009**, *38* (4), 487–493.
(14) Cuq, M. H.; Palevody, C.; Delmas, M. Fundamental study of cross-linking of collagen with chrome tanning agents in traditional and Cr.A.B processes. *J. Soc. Leather Technol. Chem.* **2000**, *83*, 233–238.
(15) Barlow, J. R. Scanning Electron-Microscopy of hides, skins and leather. *J. Am. Leather Chem. Assoc.* **1975**, *70* (3), 114–128.
(16) Dempsey, M., *Hide, Skin and Leather Defects: A Guide to Their Microscopy*; New Zealand Leather and Shoe Association: Palmerston North, New Zealand, 1984.
(17) Haines, B. M. Twentieth Procter memorial lecture: the skin before tannage - Procter's view and now. *J. Soc. Leather Technol. Chem.* **1984**, *68*, 57–70.
(18) Deb Choudhury, S.; Haverkamp, R. G.; DasGupta, S.; Norris, G. E. Effect of oxazolidine E on collagen fibril formation and stabilization of the collagen matrix. *J. Agric. Food Chem.* **2007**, *55* (17), 6813–6822.
(19) Cay, M.; Kiety, C.; Shuttleworth, A. Microfibrillar elements of the dermal matrix. *Microsc. Res. Tech.* **1997**, *38* (4), 413–427.
(20) Reich, G.; Bradt, J.; Mertig, M.; Pompe, W.; Taeger, T. Scanning probe microscopy a useful tool in leather research. *J. Soc. Leather Technol. Chem.* **1999**, *82*, 11–14.
(21) Edmonds, R. L.; Deb Choudhury, S.; Haverkamp, R. G.; Birtles, M.; Allsop, T. F.; Norris, G. E. Using proteomics, immunohistology, and atomic force microscopy to characterize surface damage to lambskins observed after enzymatic dewooling. *J. Agric. Food Chem.* **2008**, *56* (17), 7934–7941.
(22) Bernado, P.; Mylonas, E.; Petoukhov, M. V.; Blackledge, M.; Svergun, D. I. Structural characterization of flexible peoteins using small-angle X-ray scattering. *J. Am. Chem. Soc.* **2007**, *129* (17), 5656–5664.
(23) Tsutakawa, S. E.; Hura, G. L.; Frankel, K. A.; Cooper, P. K.; Tainer, J. A. Structural analysis of flexible proteins in solution by small angle x-ray scattering combined with crystallography. *J. Struct. Biol.* **2007**, *158* (2), 214–223.
(24) Cameron, G. J.; Alberts, I. L.; Laing, J. H.; Wess, T. J. Structure of type I and type III heterotypic collagen fibrils: an x-ray diffaction study. *J. Struct. Biol.* **2002**, *137*, 15–22.
(25) Sasaki, N.; Odajima, S. Stress-strain curve and youngs modulus of a collagen molecule as determined by the x-ray diffaction technique. *J. Biomech.* **1996**, *29* (5), 655–658.
(26) Burger, C.; Zhou, H. W.; Sics, I.; Hsiao, B. S.; Chu, B.; Graham, L.; Glimcher, M. J. Small-angle X-ray scattering study of intramuscular fish bone: collagen fibril superstructure determined from equidistant meridional reflections. *J. Appl. Crystallogr.* **2008**, *41*, 252–261.
(27) Cedola, A.; Mastrogiacomo, M.; Burghammer, M.; Komlev, V.; Giannoni, P.; Favia, A.; Cancedda, R.; Rustichelli, F.; Lagomarsino, S., Engineered bone from bone marrow stromal cells: A structural study by an advanced x-ray microdiffraction technique. *Phys. Med. Biol.* **2006**, *51* (6), N109−N116.
(28) Mollenhauer, J.; Aurich, M.; Muehleman, C.; Khelashvilli, G.; Irving, T. C. X-Ray Diffraction of the Molecular Substructure of Human Articular Cartilage. *Connect. Tissue Res.* **2003**, *44* (5), 201–207.
(29) Boote, C.; Sturrock, E. J.; Attenburrow, G. E.; Meek, K. M. Psuedo-affine behaviour of collagen fibres during the uniaxial deformation of leather. *J. Mater. Sci.* **2002**, *37*, 3651–3656.
(30) Sturrock, E. J.; Boote, C.; Attenburrow, G. E.; Meek, K. M. The effect of the biaxial stretching of leather on fibre orientation and tensile modulus. *J. Mater. Sci.* **2004**, *39*, 2481–2486.
(31) Cookson, D.; Kirby, N.; Knott, R.; Lee, M.; Schultz, D. Strategies for data collection and calibration with a pinhole-geometry SAXS instrument on a synchrotron beamline. *J. Synchrotron Radiat.* **2006**, *13*, 440–444.
(32) Roe, R.-J. *Methods of X-ray and Neutron Scattering in Polymer Science*; Oxford University Press: Oxford, U.K., 2000.
(33) O'Leary, D. N.; Attenburrow, G. E. Differences in strength between the grain and corium layers of leather. *J. Mater. Sci.* **1996**, *31*, 5677–5682.

Received for review February 3, 2010. Revised manuscript received March 10, 2010. Accepted March 15, 2010. The NZ Synchrotron Group Ltd. is acknowledged for travel funding. This work was supported by the Foundation for Research Science and Technology Grant No. LSRX0801.